Chapter 26
Studying Carbohydrate Self-Recognition in Marine Sponges Using Synthetic Aggregation Factor Epitopes

Johannis P. Kamerling and Adriana Carvalho de Souza

Keywords Marine sponges • *Microciona prolifera* • Aggregation factors • Carbohydrate–carbohydrate interaction • Neoglycoconjugates • Gold glyconanoparticles • Surface plasmon resonance • Transmission electron microscopy • Atomic force microscopy

Sponges (Porifera) are the simplest and earliest multicellular organisms. They do not produce complex patterned structures (i.e., organ systems). Epithelial cells (pinacocytes) line the outer surface and the internal system of openings, channels, and chambers, through which water is continuously pumped by flagellated cells called choanocytes. The generated water current supplies food particles and oxygen and removes metabolic waste products. The major part of the sponge biomass consists of a gelatinous extracellular matrix (ECM) containing a large number of highly motile cells. This part of the sponge body is called the mesohyl. The mesohyl also contains the skeletal elements of the sponge body: spicules (needle-like structures made of either silicon or calcium carbonate) and spongin (collagenous fibers).

The complex ECM observed in sponges suggests that the system that mediates cell motility and adhesion in sponges is common to all multicellular animals, thus placing the developmental role of the ECM as an ancestral homology that unites all Metazoans [1]. Interactions between cells and extracellular molecules play a fundamental role in the development of "higher" animals. The same complex set of molecules found in vertebrate ECMs also appears to be involved in cell motility and development in sponges. As sponges are the simplest multicellular animals living today, they represent an ideal model system for studying the molecular mechanisms that guide cell recognition and adhesion in ancestral Metazoans.

In 1907, Wilson pioneered the use of sponges as model animals for the study of cell adhesion. He described the existence of species-specific reaggregation of marine sponge cells that had been mechanically dissociated [2]. When sponges

J.P. Kamerling (✉)
Department of Bio-Organic Chemistry, Bijvoet Center, Utrecht University,
Padualaan 8, 3584 CH Utrecht, The Netherlands
e-mail: j.p.kamerling@chem.uu.nl

A.M. Wu (ed.), *The Molecular Immunology of Complex Carbohydrates-3*,
Advances in Experimental Medicine and Biology 705, DOI 10.1007/978-1-4419-7877-6_26,

were dissociated by squeezing through a fine-mesh cloth, single cells were produced that adhered to each other to form aggregates and eventually reorganized into perfect miniature sponges in a Ca^{2+}-dependent process [3, 4]. When dissociated cells of different species with natural pigments of contrasting colors were mixed and allowed to aggregate, it was observed that cells from the same species would combine, but not cells from different species. These results led to the conclusion that specific surface antigens are essential for adhesion. In further studies of sponge cells dissociated in Ca^{2+}-free seawater (referred to as "chemically dissociated cells"), extracellular particulates that were responsible for the species-specific cell aggregation (referred to as aggregation factors [AFs]) could be isolated [5–7]. These AFs were found to be a requirement for the aggregation of dissociated sponge cells.

In summary, sponges are thought to have evolved from their unicellular ancestors about 1 billion years ago by developing cell recognition and adhesion mechanisms for discriminating against "non-self."

26.1 Sponge AFs

Porifera AFs have been identified in several marine sponge species [5, 6, 8–10]. All of them are proteoglycan-like macromolecular complexes with molecular masses in the order of several million daltons. They are composed mainly of protein and carbohydrate in variable but substantial amounts, with a high net negative charge [11, 12]. The cell aggregation activity of marine sponge AFs depends on a Ca^{2+} concentration of about 10 mM, similar to the concentration found in seawater. Other alkaline earth cations, Mg^{2+}, Sr^{2+}, and Ba^{2+}, could not replace Ca^{2+} as an aggregation-mediating agent; however, two transition elements, Mn^{2+} and Cd^{2+}, could partially replace Ca^{2+}. Interestingly, lanthanides produced normal cell aggregation activity but only at 10- to 400-fold lower cation concentrations than Ca^{2+} [13]. Although AFs from freshwater sponges have been described and partially purified [14, 15], they are still poorly characterized. Freshwater sponge AFs are already active at Ca^{2+} concentrations of 1 mM [16], implying major differences when compared to their marine counterparts.

To confirm the role of AFs in the first step of cell recognition and adhesion, the purified proteoglycan, called glyconectin [17] or spongican [18], of three different sponge species, *Microciona prolifera*, *Halichondria panicea*, and *Cliona celata*, attached to pink, yellow, and white latex-amidine beads, respectively, were used for aggregation studies [17]. After a short rotation of the three types of proteoglycan beads in seawater with 10 mM $CaCl_2$, xenogeneic sorting and adhesion occurred. Replacement of Ca^{2+} with Mg^{2+} ions did not result in bead aggregation. In a control experiment, a mixture of yellow, pink, and white latex beads, all decorated with *M. prolifera* proteoglycan, yielded mixed orange-colored aggregates after a short rotation in the presence of 10 mM $CaCl_2$. These experiments directly showed that

species-specific proteoglycan-to-proteoglycan interactions are an example of a primordial self-recognition mechanism approaching the selectivity shown by the immunoglobulin superfamily in higher animals. The binding strength between two individual AFs in the presence of 10 mM $CaCl_2$ was measured with atomic force microscopy (AFM) [19–21]. Under physiological conditions, the average adhesive forces of individual interaction sites in two AF molecules have been estimated to be 40 ± 15 pN, whereas the average forces measured between a single pair of molecules amounted to about 125 pN, with maxima up to 400 pN [19].

Initial characterization studies showed that the *M. prolifera* AFs (MAF) and the *Geodia cydonium* AFs had a sunburst shape in the electron microscope micrographs, with a central ring structure of about 130–200 nm in diameter and 16–25 radiating arms [9, 22]. AFs extracted from *Halichondria bowerbanki*, *Terpios zeteki*, *Homalomena occulta*, and *H. panicea* had similar size and form, but a linear backbone [22, 23].

The supramolecular structure of the circular proteoglycan MAF was elucidated by using immunochemical and electrophoretical procedures, combined with AFM imaging [18, 23–25]. MAF promotes adhesion of sponge cells through a two-step process involving (1) a Ca^{2+}-dependent self-aggregation of the AF complexes and (2) a Ca^{2+}-independent binding to cell surface receptors [26]. The main proteins of MAF, MAFp3 (ranging from 30 to 50 kDa) and MAFp4 (approximately 400 kDa), are extremely polymorphic carbohydrate-containing molecules [27]. Structural studies have shown that although MAFp3 and MAFp4 are not directly related to any other described proteoglycan component, the structure of MAF has characteristics that resemble the aggregates of cartilage proteoglycan [23]. However, unlike any proteoglycan described so far, the central backbone of MAF is circularized.

The estimated total mass of MAF amounts to 2×10^4 kDa, with a carbohydrate content of 60–70% and a monosaccharide composition of glucuronic acid (GlcA):fucose (Fuc):mannose (Man):galactose (Gal):*N*-acetylglucosamine (GlcNAc) = 10:34:9:25:22 [28]. Twenty units from each of the two N-glycosylated proteins, MAFp3 and MAFp4, form the central ring and radiating arms of MAF, respectively (Fig. 26.1) [18, 23]. From the AFM images, it was estimated that each of the 20 MAFp4 arms is 140–180-nm long and has a beaded structure consisting of about 15 globules. A ~6-kDa *N*-glycan, g-6, involved in the binding of MAF to the cell receptor, is found exclusively at MAFp4. It was calculated that one MAF molecule has about 950 g-6 units [29], resulting in about 50 g-6 units in each of the MAFp4 arms. A ~200-kDa *N*-glycan, g-200, involved in the self-association of MAF [30], is found in the ring forming MAFp3. The same studies showed that one MAF has approximately 26 g-200 units. AFM imaging has shown that one or two short linear structures protrude from each of the 20 globular structures that form the ring of MAF. Whenever MAF rings were observed to form dimers or larger aggregates, they appear to be interconnected through these short chains, thus suggesting that they are g-200 glycans [23]. A simplified model of MAF-mediated sponge cell adhesion is depicted in Fig. 26.2. Ca^{2+}-dependent self-interactions of the MAFp3-bound g-200 glycan mediate self-binding of two AF complexes. MAFp3 and

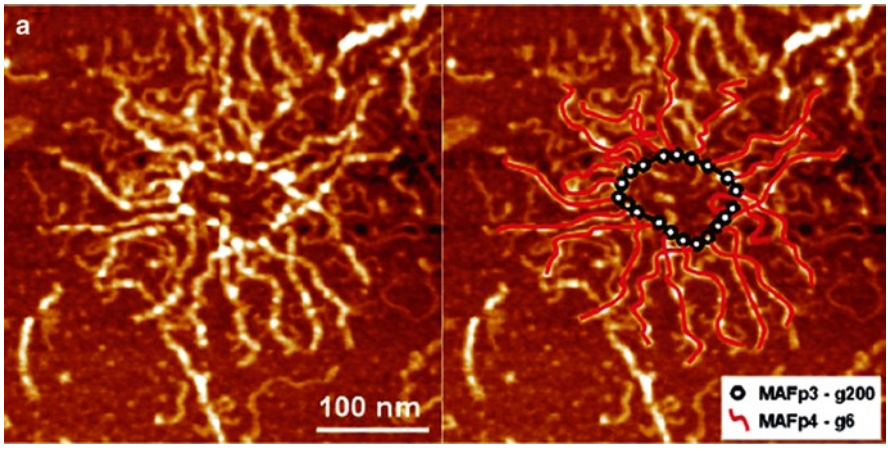

Fig. 26.1 AFM image of MAF showing the localization of MAFp3 in the *ring* (*circumferences*) and of MAFp4 in the *arms* (*lines*). From Fernàndez-Busquets and Burger [18], with permission

MAFp4 interact through a hyaluronan (HA)-like molecule [18]. The binding through the g-6 glycan to cell receptors probably involves other pericellular proteins [31–33]. For the g-200 self-interaction, a more physical model has also been proposed [21].

26.2 The *N*-Glycans of MAF

The g-6 and g-200 *N*-glycans were isolated and purified after complete pronase digestion of MAF followed by polyacrylamide gel electrophoresis, gel filtration, and ion-exchange chromatography. Composition analysis of g-6 revealed the presence of GlcA, Fuc, Man, Gal, GlcNAc, sulfate, and asparagine (Asn) in a molar ratio of 7:3:2:5:14:2:1 [29]. Carbohydrate and amino acid analysis of the purified g-200 glycan showed the presence of GlcA, Fuc, Man, Gal, GlcNAc, and Asn in a molar ratio of 32:68:2:18:19:1 [30]. It should be noted that PNGase-F is able to release the g-6 *N*-glycans of MAF but not the g-200 *N*-glycans. In a more recent study [34], monosaccharide analysis of purified MAF (glyconectin) showed the presence of GlcA, Fuc, Man, Gal, GlcNAc, GalNAc, and Gal4,6Pyr in a molar ratio of 11:28:9:29:17:1:4, a carbohydrate content of 63%, and a sulfate content of 820 mol/mol. Another recent study focused on the g-200 glycan [35] revealed the occurrence of GlcA, Fuc, Man, Gal, GlcNAc, and GalNAc in a molar ratio of 9:29:9:32:18:3.

In the context of revealing the molecular basis of MAF aggregation, two specific monoclonal antibodies raised against purified MAF, called Block 1 [28] and Block 2 [30], turned out to inhibit the Ca^{2+}-dependent self-association process without

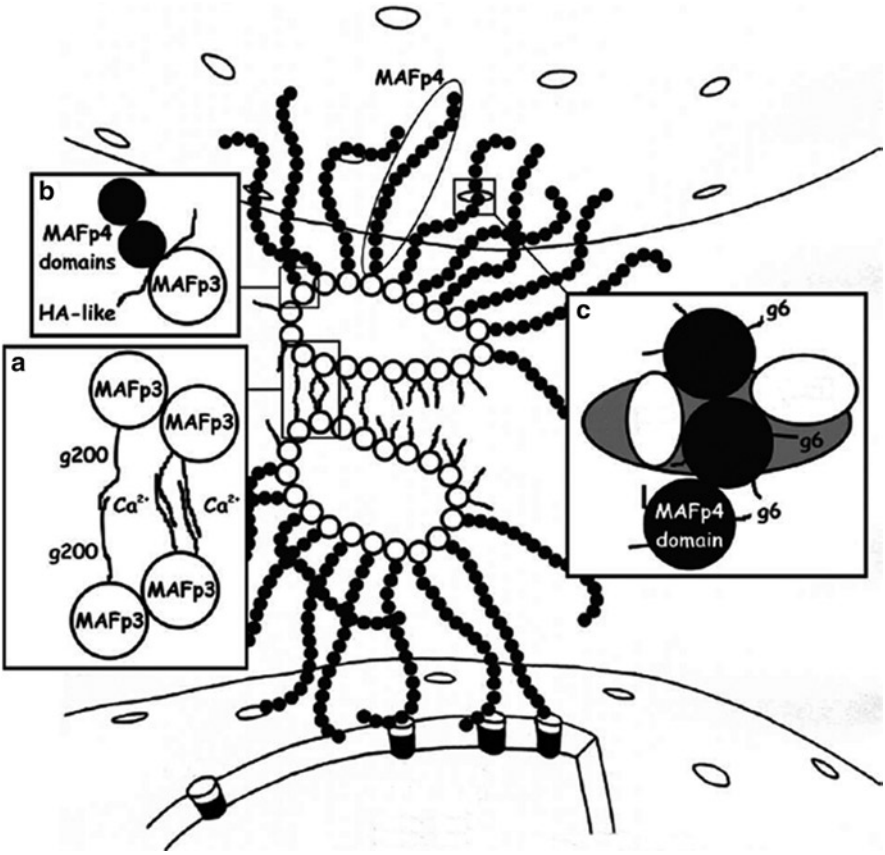

Fig. 26.2 A proposed model of the MAF-mediated sponge cell adhesion. Only half of MAFp4 and of the g-200 glycans are represented. (**a**) Ca^{2+}-dependent self-interactions of the MAFp3-bound g-200 glycan; (**b**) MAFp3 and MAFp4 interact through an HA-like molecule; (**c**) Ca^{2+}-independent binding through the g-6 glycan to cell receptors. From Fernàndez-Busquets and Burger [18], with permission

interfering with the cell-binding activity. Binding studies of the antibodies to MAF demonstrated that the highly repetitive epitopes (1,100 antigenic sites for Block 1 Fab fragments [28] and 2,500 sites for Block 2 Fab fragments [30]) were located at the acidic g-200 glycan ($M_r = 200 \times 10^3 \pm 40 \times 10^3$ kDa) [36]. However, in their monomeric form, g-200 glycans showed no measurable self-association or interaction with MAF in the presence of 10 mM $CaCl_2$, supporting data that MAF–MAF association is based on multiple low-affinity carbohydrate–carbohydrate interactions; in fact, cross-linking with glutaraldehyde into polymers led to reconstitution of the Ca^{2+}-dependent self-interaction. Also, glass aminopropyl beads coated with the g-200 glycans aggregated in the presence of 10 mM $CaCl_2$ (but not 2 mM $CaCl_2$), indicating again that the glycan, presented in a multivalent way, is capable

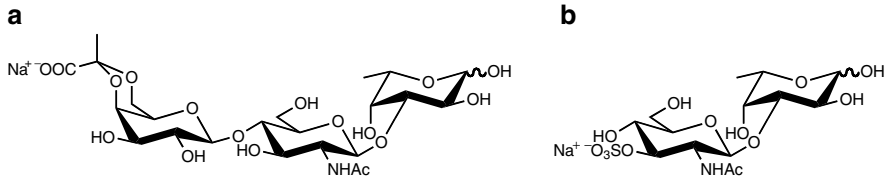

Fig. 26.3 Chemical structure of the pyruvated trisaccharide (**a**) and the sulfated disaccharide (**b**), isolated from the MAF g-200 glycan

of mediating adhesion exclusively through homophilic carbohydrate–carbohydrate interactions [30, 36]. AFM studies with the g-200 glycan in the presence of 10 mM $CaCl_2$ showed the binding forces for single glycans to be 310 ± 75 pN [36].

The epitopes, recognized by the monoclonal antibodies Block 1 and Block 2, were isolated after mild acid hydrolysis of the glycan fraction obtained via pronase digestion of MAF. Structural analysis of these epitopes, applying ^{1}H nuclear magnetic resonance (NMR) spectroscopy and mass spectrometry, showed two novel oligosaccharides, the pyruvated trisaccharide β-D-Gal*p*4,6(*R*)Pyr-(1→4)-β-D-Glc*p*NAc-(1→3)-L-Fuc*p* [37] (recognized by Block 1) and the sulfated disaccharide β-D-Glc*p*NAc3*S*-(1→3)-L-Fuc*p* [38] (recognized by Block 2) (Fig. 26.3). In the latter study, the structure of a third nonimmunoreactive oligosaccharide, α-D-Gal*p*-(1→2)-β-D-Gal*p*3*S*-(1→4)-β-D-Glc*p*NAc-(1→3)-L-Fuc*p*, was also determined [38]. In additional mass spectrometric studies of acid hydrolysates of purified MAF (glyconectin), besides GlcNAc3*S*-Fuc (see above), two other oligosaccharide fragments, Fuc-GlcNAc*S*-Fuc and GlcNAc-Fuc-GlcNAc*S*-Fuc, were identified, indicating that the sulfated disaccharide epitope may be part of a repetitive unit. Furthermore, besides Gal-Gal*S*-GlcNAc-Fuc (see above), the novel fragments Gal-Gal*S*-GlcNAc and GlcNAc-Gal*S*-Fuc were established, whereas Gal4,6Pyr-GlcNAc-Fuc (see above) was found back in minor amounts [39]. In view of the observation of preferential cleavage of glycodomains rich in acid-labile linkages (note the absence of GlcA), it has been suggested that the polysaccharide moieties are probably constituted of external acid-labile domains and an acid-resistant backbone structure. Two-dimensional NMR studies on the native MAF g-200 glycan made the assignments of α-Fuc, α-Gal, β-Gal, and β-GlcNAc possible [34], demonstrating that on the polysaccharide level, Fuc occurs in the α-configuration.

26.3 Glycans of AFs of Other Species

Besides the reports on the glycan moieties of MAF, attention was paid more recently to the mass spectrometric structural analysis of oligosaccharide fragments derived from the purified N-glycosylated AFs (glyconectins) of *C. celata* and *H. panicea* [34, 39].

Monosaccharide analysis of the AF of *C. celata* revealed the presence of Ara:Fuc:Man:Gal:GalNAc:GlcNAc:GlcA in a molar ratio of 11:31:20:12:7:13:6, with a carbohydrate content of 36% and a sulfate content of 700 mol/mol. The AF contained one major 110-kDa acidic glycan (50%) together with a mixture of smaller glycans. Proposed structures of oligosaccharides obtained via partial hydrolysis comprise HexNAc-Pent*S*-$(dHex)_{0,1}$, HexNAc-dHex*S*-$(dHex)_{0,1}$, HexNAc-Pent*S*-HexNAc-$(dHex)_{0,1}$, HexNAc-dHex*S*-HexNAc-$(dHex)_{0,1}$, and Hex-HexNAc-Pent*S*-HexNAc-dHex.

Monosaccharide analysis of the AF of *H. panicea* revealed the presence of Fuc:Man:Gal:GalNAc:GlcNAc:Gal4,6Pyr:GlcA in a molar ratio of 7:16:43:1:14:16:3, with a carbohydrate content of 21% and a sulfate content of 620 mol/mol. The AF contained one major 180-kDa acidic glycan (60%) together with a heterogeneous population of acidic glycans with sizes <10 kDa. Proposed structures of oligosaccharides obtained via partial hydrolysis comprise HexPyr-$(Hex)_{0,1}$-dHex, HexPyr-$(Hex)_{1,2,5}$, HexPyr-$(Hex)_{0,1,2}$-[Hex-]Hex, HexPyr-Hex-[HexPyr-]Hex-Hex, $(Hex)_4$-[HexPyr-]Hex, Hex-Hex-[HexPyr-]Hex-Hex, HexPyr-Hex-[Hex-]HexNAc, and HexPyr-$(Hex)_{0,1,2,3}$-HexNAc.

Another recent study focused on the glycans responsible for the carbohydrate–carbohydrate interaction in other species [35] revealed the occurrence of Fuc:Man:Gal:GalNAc:GlcNAc:GlcA in a molar ratio of 25:16:12:11:31:5 for *C. cliona*, 10:18:50:1:17:4 for *H. panicea*, and 17:14:28:2:38:2 for *Suberites fuscus*. AFM studies carried out on the glycans showed single binding of 190 ± 50 pN for *C. cliona*, 295 ± 70 pN for *H. panicea*, and 295 ± 60 pN for *S. fuscus* [36].

26.4 Carbohydrate–Carbohydrate Interactions on the Epitope Level for MAF

26.4.1 Evaluation of Simple Multivalent Systems to Explore Sulfated Disaccharide Self-Recognition on the Molecular Level

In view of the foregoing results, our group started a research project with the aim to explore the possibilities of mimicking MAF or g-200 self-interaction on the epitope, i.e., the sulfated disaccharide, level. When successful, such an approach should generate detailed information about part of the weak polyvalent carbohydrate–carbohydrate interaction in MAF on the molecular level. To this end, the sulfated disaccharide was synthesized and multivalently presented on bovine serum albumin (BSA) for ultraviolet (UV) and surface plasmon resonance (SPR) studies, on gold nanoparticles for transmission electron microscopy (TEM) studies, and on gold layers for AFM studies (Fig. 26.4).

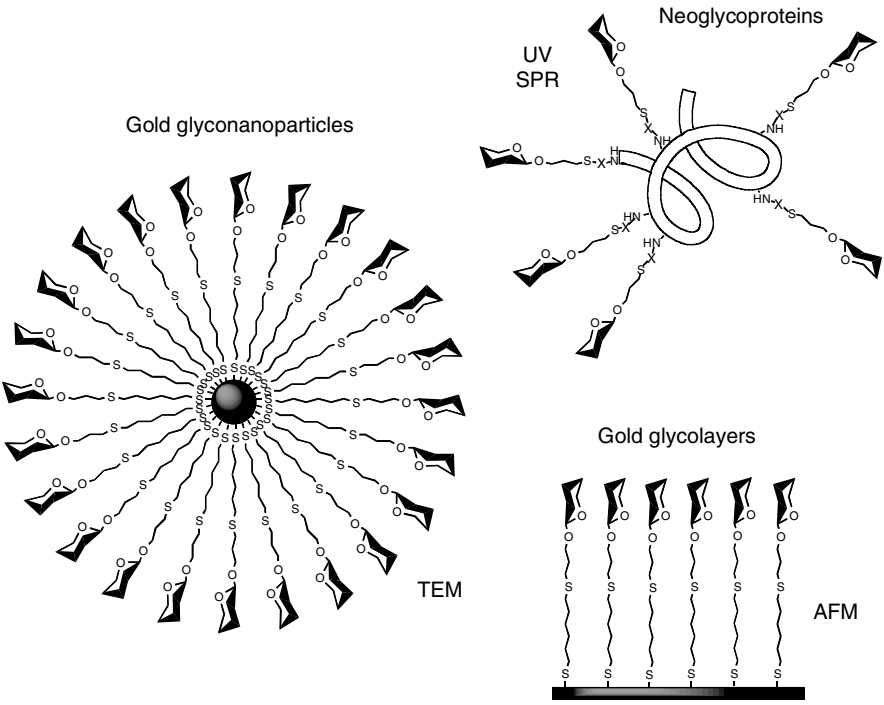

Fig. 26.4 Creation of simple multivalent systems of established MAF epitopes to explore the self-recognition of MAF on the molecular level

26.4.2 Synthesis of the Sulfated Disaccharide Epitope and Related Variants in Suitable Probe Form for Interaction Studies

The sodium salt of the synthetic disaccharide epitope was synthesized as its α-allyl glycoside, β-D-Glc*p*NAc3*S*-(1→3)-α-L-Fuc*p*-(1→O)($CH_2CH{=}CH_2$) (1a). To this end, 3-*O*-allyloxycarbonyl-2-deoxy-4,6-*O*-isopropylidene-2-phtalimido-β-D-glucopyranosyl trichloroacetimidate was coupled with allyl 2,4-di-*O*-benzoyl-α-L-fucopyranoside using trimethylsilyl trifluoromethanesulfonate as a catalyst. The formed disaccharide derivative was deisopropylidenated, then acetylated, deallyloxycarbonylated, sulfated, deacylated, and finally *N*-acetylated, yielding the title compound [40].

In a similar way, a series of six variants of the synthetic disaccharide epitope were prepared, namely, β-D-Glc*p*NAc3*S*-(1→3)-β-L-Fuc*p*-(1→O)($CH_2CH{=}CH_2$) (1b); β-D-Glc*p*NAc3*S*-(1→O)($CH_2CH{=}CH_2$) (2); α-L-Fuc*p*-(1→O)($CH_2CH{=}CH_2$) (3); β-D-Glc*p*NAc3*S*-(1→3)-α-L-Gal*p*-(1→O)($CH_2CH{=}CH_2$) (4); β-D-Glc*p*NAc-(1→3)-α-L-Fuc*p*-(1→O)($CH_2CH{=}CH_2$) (5); and β-D-Glc*p*3*S*-(1→3)-α-L-Fuc*p*-(1→O)($CH_2CH{=}CH_2$) (6) [41].

For the aimed disaccharide–disaccharide interaction studies, two different probes were constructed, namely, BSA glycoconjugates and gold glyconanoparticles (GNPs).

To prepare the BSA conjugate, the synthetic disaccharide epitope 1a was converted into the corresponding 3-(2-aminoethylthio)propyl glycoside 1a-NH_2 by reaction with cysteamine under UV irradiation, and the formed amino-group-containing glycoside was coupled to BSA using diethyl squarate as the bivalent linker (→ 1a-BSA). MALDI-TOF MS indicated a decoration of, on average, 7.8 hapten molecules per molecule of BSA (Fig. 26.5) [40].

For the preparation of the GNPs, the first step comprised the conversion of the synthetic disaccharide epitope 1a into the corresponding 3-(6-mercaptohexylthio) propyl glycoside 1a-SH (Fig. 26.6). The conjugation to gold was realized via a

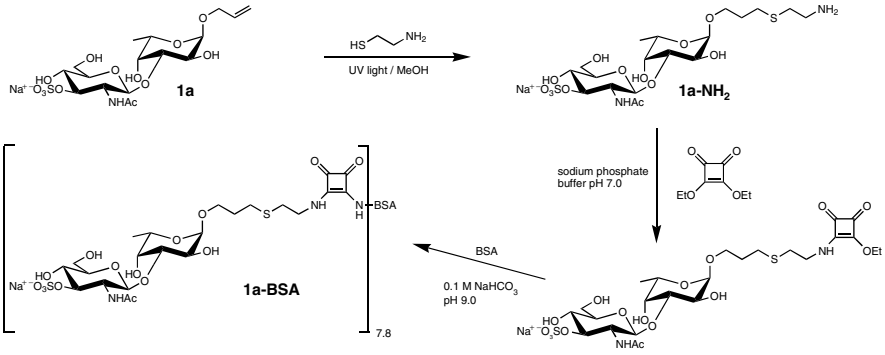

Fig. 26.5 Synthesis of the sulfated disaccharide epitope conjugated with BSA (1a-BSA)

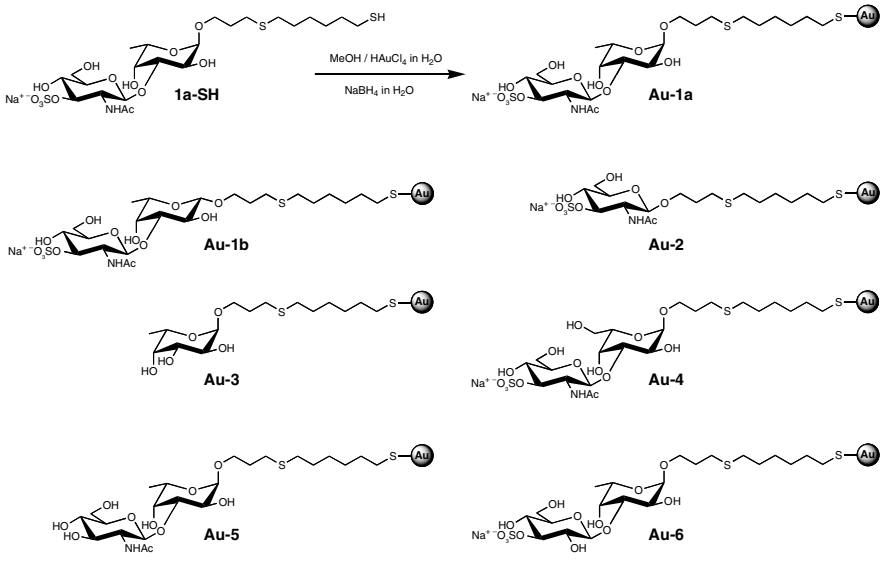

Fig. 26.6 Preparation of GNPs. Synthesis of Au-1a and structures of the GNPs Au-1a/b to Au-6

reduction of tetrachloroauric anion with $NaBH_4$ in the presence of 1a-SH (→ Au-1a). The formed particles were insoluble in methanol but soluble in water. Characterization was carried out by ^1H NMR spectroscopy, monosaccharide analysis, and TEM. Similarly, the six variants 1b and 2–6 were transformed via the thiolated intermediates into the GNPs Au-1b and Au-2 to Au-6, respectively (Fig. 26.6) [41]. To give an impression of the characteristics of the GNPs, Table 26.1 summarizes the averaged diameter of the particles, their dispersity, their carbohydrate content, their number of gold atoms, and their number of carbohydrate ligands.

26.4.3 *Interaction Studies with the Sulfated Disaccharide Probe Using UV Spectroscopy*

The aggregation behavior of β-D-Glc*p*NAc3*S*-(1→3)-α-L-Fuc*p*-(1→O), when multivalently presented on BSA (Fig. 26.5, 1a-BSA), was investigated by monitoring the absorbance, or alternatively the turbidity, of 10 μM conjugate in 20 mM Tris–HCl buffer, pH 7.4/500 mM NaCl (the concentration found in seawater) in the presence and in the absence of 10 mM $CaCl_2$ (the Ca^{2+} concentration commonly found in seawater) or $MgCl_2$ [42]. The experiments were carried out at three different wavelengths: 340, 440, and 600 nm, for 100 min. Although, in theory, the turbidity measurement should be independent of the wavelength chosen, three wavelengths were selected to ensure that the protein part of the neoglycoprotein did not disturb the results. BSA and Glc6*S*-containing BSA conjugate (Glc6*S*-BSA; loading on average 9.7 mol/mol) were included as reference compounds. As is evident from Fig. 26.7a (340 nm), on addition of Ca^{2+}-ions, a rapid decrease in absorbance takes place, which correlates with a rapid aggregation of the conjugate; similar results were found at 440 and 600 nm. The aggregation phenomenon was not observed in the presence of Mg^{2+}-ions (Fig. 26.7b). The reference compounds did not show the aggregation phenomenon, indicating the specificity of the effect. In fact, the UV studies matched those carried out with *M. prolifera* cells and MAF-coated beads.

Table 26.1 Specific features of prepared GNPs

GNPs	D_{core} (nm)	Dispersity (%)	% CHO	# Gold atoms	# CHO ligands
Au-1a	1.82 ± 0.8	44	36	201	33
Au-1b	1.71 ± 0.6	35	40	201	39
Au-2	1.51 ± 0.6	40	23	116	13
Au-3	1.80 ± 0.7	39	22	201	31
Au-4	1.80 ± 0.6	33	39	201	37
Au-5	1.63 ± 0.6	37	41	140	34
Au-6	1.55 ± 0.6	39	37	116	22

Survey of mean diameter measurements, monosaccharide analyses (%CHO), calculations of atoms, and calculation of the number of ligands per core for GNPs Au-1a/1b to Au-6

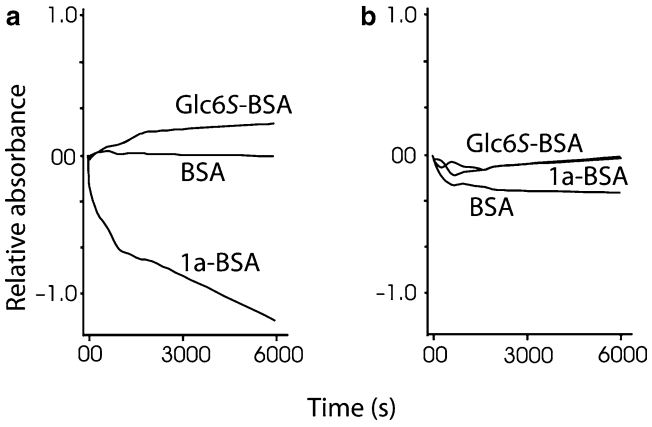

Fig. 26.7 UV analysis of the aggregation behavior of 1a-BSA, Glc6*S*-BSA, and BSA, in the presence of either 10 mM $CaCl_2$ (**a**) or 10 mM $MgCl_2$ (**b**). On addition of the divalent cation (1 M, 5 μL) to a solution (10 μM, 495 μL) of the test molecule, the tube was mixed, and the absorbance was zeroed. The absorbance was then measured at 340 nm for 6,000 s

26.4.4 Interaction Studies with the Sulfated Disaccharide Probe Using SPR Spectroscopy

Further insight into the carbohydrate–carbohydrate interactions mediating MAF aggregation was obtained by SPR [42]. This detection principle allows the interaction between one substance bound to a gold surface (substrate) and another in solution flowing across the surface (analyte) to be monitored. An increase in the SPR response denotes an increase in surface concentration, and hence, an interaction. For the experiments, carboxymethylated dextran-coated gold surfaces (CM5 sensor chips) were used. The analyses were performed in 20 mM Tris–HCl buffer, pH 7.4/500 mM NaCl, either with or without 10 mM $CaCl_2$, $MgCl_2$, or $MnCl_2$. To account for nonspecific protein–protein and protein–carbohydrate interactions within the whole system, unmodified, ethanolamine-neutralized, and BSA-coated surfaces were used as control substrate surfaces; the substrate loadings of 1a-BSA and BSA were around 10,000 RU. In a series of 500-s association/dissociation experiments (concentration range for the analyte between 10 and 0.31 μM, in two-fold dilutions), it turned out that in the absence of Ca^{2+}-ions, BSA (substrate) did not interact with BSA (analyte), and 1a-BSA (substrate) did not interact with 1a-BSA (analyte). BSA (substrate) and 1a-BSA (analyte) as well as 1a-BSA (substrate) and BSA (analyte) showed low affinities for each other, due to carbohydrate–protein interactions. In the presence of Ca^{2+}-ions, the couples BSA (substrate)–BSA (analyte), BSA (substrate)–1a-BSA (analyte), and 1a-BSA (substrate)–BSA (analyte) showed a similar behavior as in the absence of Ca^{2+} ions. However, in the presence of Ca^{2+}-ions, the couple 1a-BSA (substrate)–1a-BSA (analyte) revealed a completely different behavior, whereby the binding response is beginning to ascend to infinity

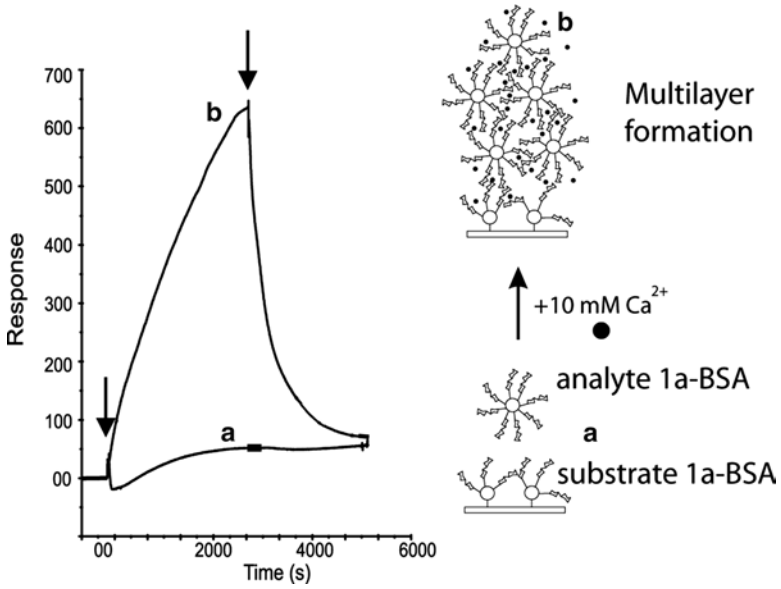

Fig. 26.8 Illustration of the polyvalent multilayer formation of 1a-BSA (10 μM), as detected by SPR in a 40-min association/dissociation experiment. Bound substrate and flowing analyte are 1a-BSA; injection of analyte in the absence (**a**) and in the presence (**b**) of 10 mM $CaCl_2$. *Arrows* in the sensorgrams indicate commencement of association and dissociation

in a linear fashion. Such a behavior is indicative of a low-affinity polyvalent binding mechanism for which saturation of the surface cannot be attained, and multilayer formation is induced ($K_a \sim 10^5\ M^{-1}$). Overall the association/dissociation process of 1a-BSA in the presence of Ca^{2+}-ions in the analyte is a rapid multiple event.

As an illustration, sensorgrams of 40-min association/dissociation experiments are presented in Fig. 26.8. The various SPR data clearly showed that the conjugated sulfated disaccharide 1a-BSA interacts with itself in the presence of Ca^{2+}-ions not simply through electrostatic interaction, since Glc6*S*-BSA and GlcA-BSA analyzed with the same procedure did not show any self-recognition. As shown earlier on the polymer level for *M. prolifera* cells and MAF-coated beads, replacement of Ca^{2+}-ions by Mg^{2+} or Mn^{2+} ions eradicated completely the self-recognition of the sulfated disaccharide.

26.4.5 Interaction Studies with the Sulfated Disaccharide Probe and Related Variant Probes Using TEM

In a quite different approach, the usefulness of water-soluble GNPs combined with TEM was explored [43]. Aliquots of the GNP probes Au-1a/1b to Au-6 (Fig. 26.6)

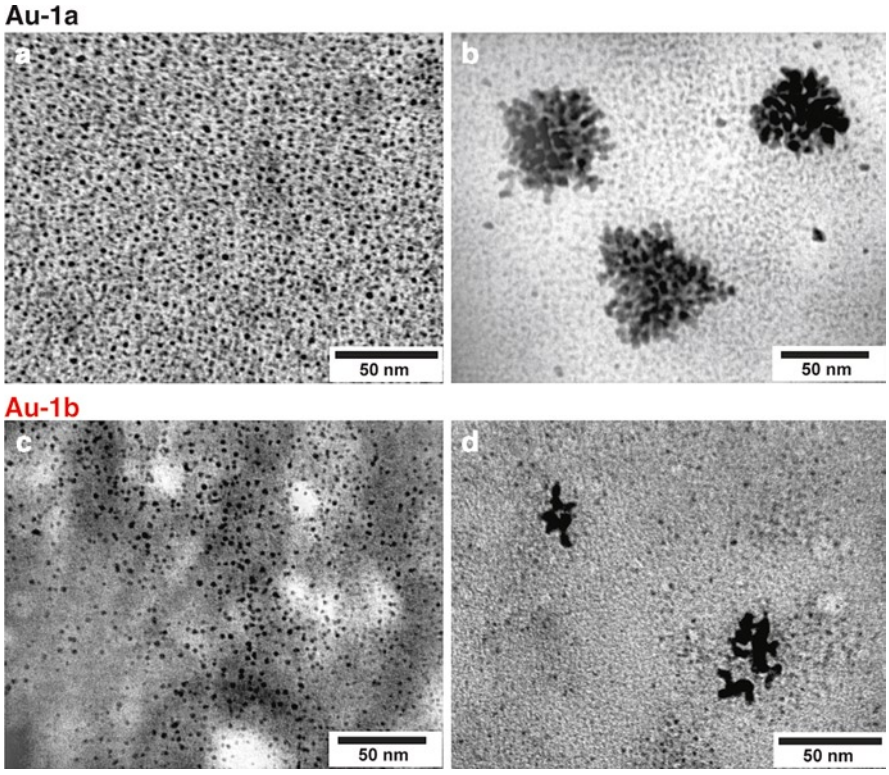

Fig. 26.9 TEM of GNPs. TEM images of Au-1a and Au-1b (0.1 mg/mL) in water (**a** and **c**) and after 16-h incubation in 10 mM $CaCl_2$ (**b** and **d**)

in aqueous solution (0.1 mg/mL) in the presence and absence of 10 mM $CaCl_2$ were placed onto copper grids and subsequently observed under the microscope.

The TEM micrographs of all GNP probes in water (no $CaCl_2$) showed uniformly dispersed nanodots throughout the grid surface (e.g., Fig. 26.9a, c). However, repetition of the experiments in $CaCl_2$ revealed that the Au-1a and Au-1b GNPs form clear aggregates (Fig. 26.9b, d); the Au-2 to Au-6 GNPs gave rise to the same uniformly dispersed nanodots as seen in the absence of Ca^{2+}-ions. As is clear from Fig. 26.9, there is a striking difference in size between the aggregates of Au-1a and Au-1b. After 16 h of incubation, the Au-1a aggregates reached a diameter of approximately 100 nm, whereas the Au-1b aggregates did not grow larger than 15 nm. So, the α-configuration of the Fuc residue in Au-1a must be responsible for the stronger self-recognition, a configuration that is also present in the native polysaccharide. Addition of ethylenediaminetetraacetic acid (final concentration 50 mM) to the Au-1a aggregates dispersed the aggregates completely, confirming the dependency of the carbohydrate–carbohydrate self-recognition on Ca^{2+}-ions. Incubation of Au-1a in 10 mM $MgCl_2$ (0.1 mg/mL) did not result in aggregate formation, again in agreement with the *M. prolifera* cells and MAF-coated beads data.

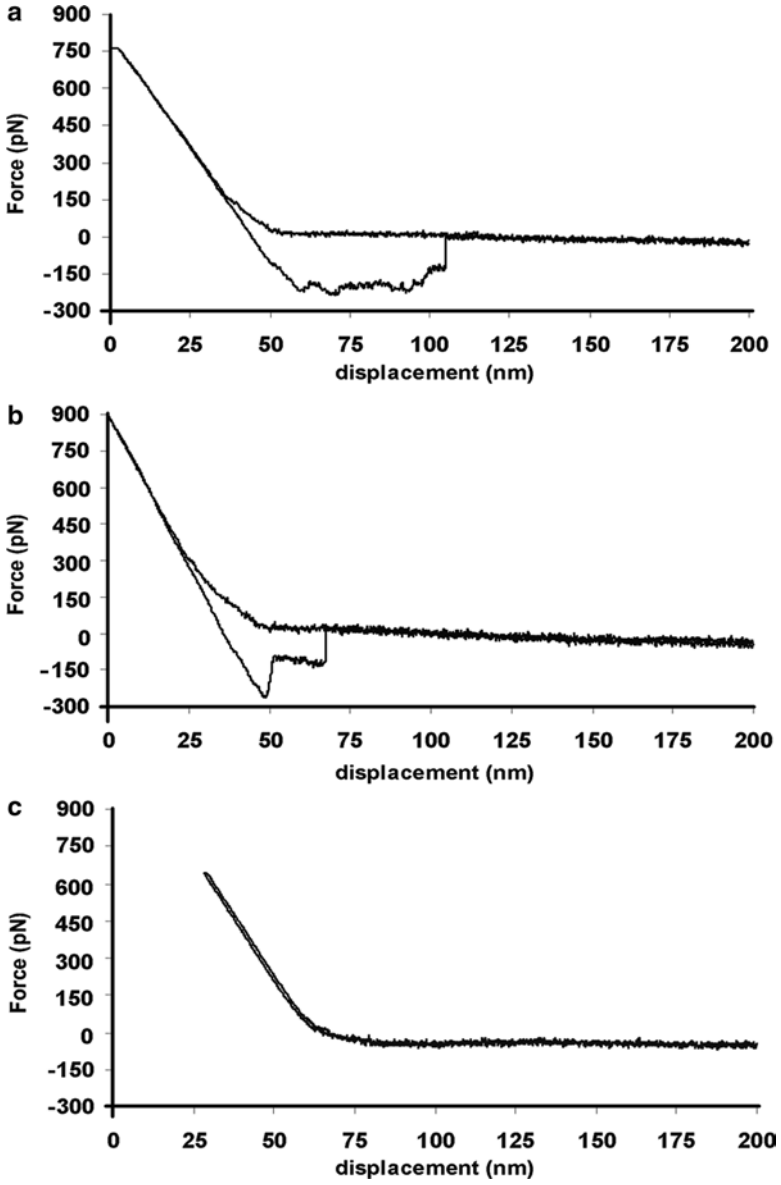

Fig. 26.10 AFM of self-assembled glycomonolayers. Typical AFM force–distance curves obtained with a 1a-SH functionalized gold tip and sample in 10 mM $CaCl_2$ (**a** and **b**). Typical AFM force–distance curve obtained with a 1a-SH functionalized gold tip and sample in water (**c**)

The fact that Au-2 and Au-3 (the two monosaccharide constituents) did not give rise to aggregation in the presence of Ca^{2+}-ions indicated the importance of the disaccharide as a whole in the self-interaction process. Taking into account the negative TEM results for Au-4 (L-Fuc replaced by L-Gal), Au-5 (D-GlcNAc3*S* replaced by D-GlcNAc), and Au-6 (D-GlcNAc3*S* replaced by D-Glc3*S*), it can be stated that the combined occurrence of the sulfate and the *N*-acetyl group in GlcN together with the methyl group in Fuc seems to be essential to the self-recognition phenomenon.

26.4.6 Interaction Studies with the Sulfated Disaccharide Probe Using AFM

To determine the binding force of the carbohydrate–carbohydrate interaction of the sulfated disaccharide probe 1a-SH, AFM was applied [44]. Measurements were carried out with the gold tip and gold sample coated with a self-assembling monolayer of 1a-SH. Control experiments were performed with an unfunctionalized gold tip and a functionalized gold sample, and vice versa, and both an unfunctionalized gold tip and gold sample. In Fig. 26.10a, b, force–distance curves are presented, made in the presence of 10 mM $CaCl_2$; in fact, these curves represent 2 out of over 300 approach–retract cycles, performed in different areas of the surface sample. Typical features for interactions between biomolecules are seen with, in some cases, multiple stepwise break processes. Autocorrelation analysis of a histogram, derived from more than 300 measured final rupture forces, yielded a force quantum of 30 ± 6 pN, attributed to the interaction of a single 1a-SH pair. Control experiments in water, showing no interaction (Fig. 26.10c), confirmed that the adhesion force of 30 pN corresponds to the Ca^{2+}-dependent sulfated disaccharide self-recognition.

26.5 Conclusions

This chapter summarizes UV, SPR, TEM, and AFM studies carried out with a multivalently presented sulfated disaccharide MAF epitope of *M. prolifera* marine sponge cells. To this end, BSA conjugates and GNPs were explored. It turned out that no self-recognition was observed for the sulfated disaccharide in water and aqueous NaCl. In the presence of Ca^{2+} ions, all approaches supported a self-recognition on the disaccharide level, whereas in the presence of Mg^{2+} and Mn^{2+} ions, no self-recognition was observed. In the presence of Cd^{2+} ions, a weak self-recognition is detected. The negative results with the monosaccharide (α-L-Fuc and β-D-GlcNAc3*S*) and disaccharide (L-Fuc → L-Gal, D-GlcNAc3*S* → D-GlcNAc, D-GlcNAc3*S* → D-Glc3*S*) variants shed further light on the high specificity of the self-interaction.

It is stated that Ca^{2+} ions have an essential role in the approach and organization of the saccharide moieties of the g-200-derived sulfated disaccharide. After coordination with Ca^{2+}, the sulfated disaccharide reaches an adequate conformation, wherein other interactions, such as hydrophobic contacts, can stabilize the whole complex. The α-configuration of Fuc is important for optimal aggregation (appropriate hydrophobic contacts).

References

1. Morris PJ (1993) The developmental role of the extracellular matrix suggests a monophyletic origin of the kingdom Animalia. Evolution 47:152–165
2. Wilson HV (1907) On some phenomena of coalescence and regeneration in sponges. J Exp Zool 5:245–258
3. Galtsoff PS (1925) Regeneration after dissociation: an experimental study on sponges I. J Exp Zool 42:183–221
4. Galtsoff PS (1925) Regeneration after dissociation: an experimental study on sponges II. J Exp Zool 42:223–251
5. Humphreys T (1963) Chemical dissolution and *in vitro* reconstruction of sponge cell adhesions I. Isolation and functional demonstration of the components involved. Dev Biol 53:27–47
6. Moscona AA (1963) Studies on cell aggregation: demonstration of materials with selective cell-binding activity. Proc Natl Acad Sci USA 49:742–747
7. Humphreys T (1965) Cell surface components participating in aggregation: evidence for a new cell particulate. Exp Cell Res 40:539–543
8. Margolaish E, Schenck JR, Hargie MP, Burokas S, Richter WR, Barlow GH, Moscona AA (1965) Characterization of specific cell aggregating materials from sponge cells. Biochem Biophys Res Commun 20:383–388
9. Müller WE, Zahn RK (1973) Purification and characterization of a species-specific aggregation factor in sponges. Exp Cell Res 80:95–104
10. Müller WE, Beyer R, Pondeljak V, Müller I, Zahn RK (1978) Species-specific aggregation factor in sponges XIII. Entire and core structure of the large circular proteid particle from *Geodia cydonium*. Tissue Cell 10:191–199
11. Henkart P, Humphreys S, Humphreys T (1973) Characterization of sponge aggregation factor. A unique proteoglycan complex. Biochemistry 12:3045–3050
12. Misevic GN, Burger MM (1986) Reconstitution of high cell binding affinity of a marine sponge aggregation factor by cross-linking of small low affinity fragments into a large polyvalent polymer. J Biol Chem 261:2853–2859
13. Rice DJ, Humphreys T (1983) Two Ca^{2+} functions are demonstrated by the substitution of specific divalent and lanthanide cations for the Ca^{2+} required by the aggregation factor complex from the marine sponge, *Microciona prolifera*. J Biol Chem 258:6394–6399
14. Curtis AS, Van de Vyver G (1971) The control of cell adhesion in a morphogenetic system. J Embryol Exp Morphol 26:295–312
15. Van de Vyver G (1975) Phenomena of cellular recognition in sponges. Curr Top Dev Biol 10:123–140
16. Rasmont R (1961) Une technique de culture des éponges d'eau douce en milieu controlé. Ann Soc R Zool Belg 91:147–155
17. Popescu O, Misevic GN (1997) Self-recognition by proteoglycans. Nature 386:231–232
18. Fernàndez-Busquets X, Burger MM (2003) Circular proteoglycans from sponges: first members of the spongican family. Cell Mol Life Sci 60:88–112

19. Dammer U, Popescu O, Wagner P, Anselmetti D, Güntherodt HJ, Misevic GN (1995) Binding strength between cell adhesion proteoglycans measured by atomic force microscopy. Science 267:1173–1175
20. Fritz J, Anselmetti D, Jarchow J, Fernàndez-Busquets X (1997) Probing single bio-molecules with atomic force microscopy. J Struct Biol 119:165–171
21. Popescu O, Checiu I, Gherghel P, Simon Z, Misevic GN (2003) Quantitative and qualitative approach of glycan-glycan interactions in marine sponges. Biochimie 85:181–188
22. Humphreys S, Humphreys T, Sano J (1977) Organization and polysaccharides of sponge aggregation factor. J Supramol Struct 7:339–351
23. Jarchow J, Fritz J, Anselmetti D, Calabro A, Hascall VC, Gerosa D, Burger MM, Fernàndez-Busquets X (2000) Supramolecular structure of a new family of circular proteoglycans mediating cell adhesion in sponges. J Struct Biol 132:95–105
24. Fernàndez-Busquets X, Burger MM (1999) Cell adhesion and histocompatibility in sponges. Microsc Res Tech 44:204–218
25. Bucior I, Burger MM (2004) Carbohydrate-carbohydrate interactions in cell recognition. Curr Opin Struct Biol 14:631–637
26. Jumblatt JE, Schlup V, Burger MM (1980) Cell-cell recognition: specific binding of *Microciona* sponge aggregation factor to homotypic cells and the role of calcium ions. Biochemistry 19:1038–1042
27. Fernàndez-Busquets X, Burger MM (1997) The main protein of the aggregation factor responsible for species-specific cell adhesion in the marine sponge *Microciona prolifera* is highly polymorphic. J Biol Chem 272:27839–27847
28. Misevic GN, Finne J, Burger MM (1987) Involvement of carbohydrates as multiple low affinity interaction sites in the self-association of the aggregation factor from the marine sponge *Microciona prolifera*. J Biol Chem 262:5870–5877
29. Misevic GN, Burger MM (1990) The species-specific cell-binding site of the aggregation factor from the sponge *Microciona prolifera* is a highly repetitive novel glycan containing glucuronic acid, fucose, and mannose. J Biol Chem 265:20577–20584
30. Misevic GN, Burger MM (1993) Carbohydrate-carbohydrate interactions of a novel acidic glycan can mediate sponge cell adhesion. J Biol Chem 268:4922–4929
31. Varner JA, Burger MM, Kaufman JF (1988) Two cell surface proteins bind the sponge *Microciona prolifera* aggregation factor. J Biol Chem 263:8498–8508
32. Varner JA (1995) Cell adhesion in sponges: potentiation by a cell surface 68 kDa proteoglycan-binding protein. J Cell Sci 108:3119–3126
33. Varner JA (1996) Isolation of a sponge-derived extracellular matrix adhesion protein. J Biol Chem 271:16119–16125
34. Misevic GN, Guerardel Y, Sumanovski LT, Slomianny MC, Demarty M, Ripoll C, Karamanos Y, Maes E, Popescu O, Strecker G (2004) Molecular recognition between glyconectins as an adhesion self-assembly pathway to multicellularity. J Biol Chem 279:15579–15590
35. Bucior I, Burger MM (2004) Carbohydrate-carbohydrate interaction as a major force initiating cell-cell recognition. Glycoconj J 21:111–123
36. Bucior I, Scheuring S, Engel A, Burger MM (2004) Carbohydrate-carbohydrate interaction provides adhesion force and specificity for cellular recognition. J Cell Biol 165:529–537
37. Spillmann D, Hård K, Thomas-Oates J, Vliegenthart JFG, Misevic G, Burger MM, Finne J (1993) Characterization of a novel pyruvylated carbohydrate unit implicated in the cell aggregation of the marine sponge *Microciona prolifera*. J Biol Chem 268:13378–13387
38. Spillmann D, Thomas-Oates JE, van Kuik JA, Vliegenthart JFG, Misevic G, Burger MM, Finne J (1995) Characterization of a novel sulfated carbohydrate unit implicated in the carbohydrate-carbohydrate-mediated cell aggregation of the marine sponge *Microciona prolifera*. J Biol Chem 270:5089–5097
39. Guerardel Y, Czeszak X, Sumanovski LT, Karamanos Y, Popescu O, Strecker G, Misevic GN (2004) Molecular fingerprinting of carbohydrate structure phenotypes of three porifera proteoglycan-like glyconectins. J Biol Chem 279:15591–15603

40. Vermeer HJ, Kamerling JP, Vliegenthart JFG (2000) Synthesis and conjugation of a sulfated disaccharide involved in the aggregation process of the marine sponge *Microciona prolifera*. Tetrahedron Asymmetry 11:539–547
41. Carvalho de Souza A, Halkes KM, Meeldijk JD, Verkleij AJ, Vliegenthart JFG, Kamerling JP (2004) Synthesis of gold glyconanoparticles: possible probes for the exploration of carbohydrate-mediated self-recognition of marine sponge cells. Eur J Org Chem 2004:4323–4339
42. Haseley SR, Vermeer HJ, Kamerling JP, Vliegenthart JFG (2001) Carbohydrate self-recognition mediates marine sponge cellular adhesion. Proc Natl Acad Sci USA 98:9419–9424
43. Carvalho de Souza A, Halkes KM, Meeldijk JD, Verkleij AJ, Vliegenthart JFG, Kamerling JP (2005) Gold glyconanoparticles as probes to explore the carbohydrate-mediated self-recognition of marine sponge cells. ChemBioChem 6:828–831
44. de Carvalho Souza A, Ganchev DN, Snel MME, van der Eerden JPJM, Vliegenthart JFG, Kamerling JP (2009) Adhesion forces in the self-recognition of oligosaccharide epitopes of the proteoglycan aggregation factor of the marine sponge *Microciona prolifera*. Glycoconj J 26:457–465